Materials Physics and Mechanics 42 (2019) 265-271 Received: May 27, 2019

# EVOLUTION OF THE DROPLET SHAPE IN THE VAPOR-LIQUID-SOLID GROWTH OF III-V NANOWIRES UNDER VARYING MATERIAL FLUXES

**V.G. Dubrovskii**[1,2,*], **A.S. Sokolovskii**[1]

[1]ITMO University, Kronverkskiy pr. 49, 197101 St. Petersburg, Russia

[2]Ioffe Institute RAS, Politekhnicheskaya 26, 194021 St. Petersburg, Russia

*e-mail: dubrovskii@mail.ioffe.ru

**Abstract.** We present a model for the time evolution of the shape of a droplet catalyzing the vapor-liquid-solid growth of III-V semiconductor nanowires under varying group III or group V fluxes. Under the assumption of a constant radius of the nanowire top, the model gives the time dependence of the droplet contact angle. These results can be used for the fine tuning of the droplet shape, which affects the preferred crystal phase (zincblende or wurtzite) of III-V nanowires.

**Keywords:** Catalyst droplet, vapor-liquid-solid growth, III-V nanowires

## 1. Introduction

III-V nanowires (NWs) and heterostructures within such NWs [1,2] offer otherwise unattainable functionalities of optoelectronic devices, in particular those monolithically integrated with silicon electronic platform. Very efficient elastic stress relaxation on the NW lateral sidewalls enable dislocation-free growth of lattice-mismatched III-V NW heterostructures [3,4] on silicon substrates [4], which is challenging in planar layers and even quantum dots [5]. Most III-V NWs are obtained via the vapor-liquid-solid (VLS) method [6] with a catalyst droplet promoting the NW growth in vertical direction. Catalyst metals are usually gold [6-10] or a group III metal [11-13] in the self-catalyzed approach. One of the most interesting features of VLS NWs of zincblende (ZB) III-V materials is their ability to form in the wurtzite (WZ) phase (see, for example, Ref. [14] for a review). This ZB-WZ polytypism in III-V NWs has been of great interest for a long time. As a result, several methods have been developed to controllably switch the crystal phase of III-V NWs by the growth parameter tuning, for example, by changing the V/III flux ratio [15]. The so-called crystal phase quantum dots, or ZB/WZ heterostructures have thus become possible, with extremely abrupt interfaces and interesting optical properties [16]. However, some aspects require a deeper understanding, in particular, the role of the droplet contact angle in the crystal phase selection and how the droplet shape changes under varying material fluxes.

The first models of polytypism in III-V NWs were originally developed for vertical facets and planar liquid-solid interface [17-19], which is the natural geometry of VLS NWs. However, more recent *in situ* experimental observations of III-V NW growth in a transmission electron microscope [20-22] revealed the presence of truncated facets at the growth interface of GaP [21] and GaAs [22] NWs. It has been shown that the morphology of gold-catalyzed GaAs NWs critically depends on the contact angle of the catalyst droplet, with the growth front being planar at smaller and truncated at larger contact angles [22]. According to Tersoff *et al.* [20,21] the crystal phase of truncated III-V NWs should be pure ZB. This is related to the stability of truncated facet such that new islands nucleate at the liquid-solid

http://dx.doi.org/10.18720/MPM.4232019_1

interface rather than at the triple phase line where the vapor, liquid and solid phases meet. Nucleation at the triple phase line is indeed the necessary condition for the WZ phase formation according to Glas *et al.* [17]. This explains the importance of the contact angle, which is currently considered as the most important parameter controlling the crystal phase selection in III-V NWs [22,23].

We have recently presented a stationary model for the droplet shape under different group III and V fluxes [24]. Here, we develop a non-stationary generalization of the model which yields the time dependence of the droplet contact angle under varying material fluxes.

## 2. Model

Let us consider the most general case of a ternary Au-III-V droplet catalyzing the VLS growth of a binary III-V NW. Introducing the numbers $N_k$ of group III ($k=3$), group V ($k=5$) and gold ($k=Au$) atoms in the liquid droplet, their sum is related to the radius of the NW top $R$ and the contact angle of the droplet $\beta$ as

$$N_3(t)+N_5(t)+N_{Au}=\frac{\pi R^3(t)}{3\Omega_L}f[\beta(t)]. \tag{1}$$

Here, $\Omega_L$ is the average elementary volume per atom in the liquid phase ($\Omega_L \cong 0.02$ nm$^3$ for Au-Ga-As alloy [2]) and

$$f(\beta)=\frac{(1-\cos\beta)(2+\cos\beta)}{(1+\cos\beta)\sin\beta} \tag{2}$$

is the geometrical function of the contact angle. These expressions are written for cylindrical NW and spherical cap droplet seated on the NW top. According to Eq. (1), the number of gold atoms in the droplet is fixed ($N_{Au}=const$), while both $N_3$ and $N_5$ can change with time, leading to the time dependence of the NW top radius $R$, or the contact angle $\beta$, or both $R$ and $\beta$ in the general case.

Assuming that (i) the number of group III atoms in the droplet changes in time due to the direct impingement flux and NW growth, without surface diffusion from the NW sidewalls [2,9], (ii) there is no desorption of group III atoms from the droplet at a growth temperature, and (iii) the NW growth is mononuclear [2,14,17,18], the kinetic equations describing the time evolution of $N_3$ and $N_5$ are given by [2,24]:

$$\frac{dN_3}{dt}=\frac{\pi R^2}{\Omega_S}\left[\chi_3(t)v_3(t)-\pi R^2 hJ(t)\right], \tag{3}$$

$$\frac{dN_5}{dt}=\frac{\pi R^2}{\Omega_S}\left[\chi_5(t)v_5(t)-\frac{2}{[1+\cos\beta(t)]}v_5^{des}\exp(n\mu_5)-\pi R^2 hJ(t)\right]. \tag{4}$$

Here, $\Omega_S$ is elementary volume per III-V pair in the solid phase ($\Omega_S$ = 0.0452 nm$^3$ for ZB GaAs [14]), $\chi_k(\beta)$ are the geometrical coefficients ($\chi_k=2/(1+\cos\beta)$ for both growth species in vapor deposition techniques, while in the directional deposition methods such as molecular beam epitaxy they are given in Ref. [25]), $v_k(t)$ are the time-dependent vapor fluxes, including possible re-emission (in nm/s), $h$ is the height of a monolayer ($h=0.326$ nm for ZB GaAs [14] growing in <111> direction), $v_5^{des}$ is the pre-exponent of the desorption term for group V atoms, $\mu_5$ is the chemical potential of group V atoms in the liquid phase in thermal units, and $n=2$ is group V atoms desorb as dimers (As$_2$ or P$_2$). The $J(t)$ is the nucleation rate of two-dimensional islands on the NW top facet [in 1/(nm$^2$s)] (Refs. [2,24]).

For large enough $\beta$ or small incident angles of the group III and V beams with respect to the vertical, the result of Ref. [25] for $\chi_k$ is reduced to $\chi_k = 1/\sin^2(\beta)$ for both growth species.

Very important results of Ref. [26] revealed the existence of the two stable contact angles of self-catalyzed GaAs NWs, one around 90-95° and the other around 130°, corresponding to the NW growth with shrinking or extending the top radius. Between these two stable angles, the droplet changes its volume by changing the contact angle at a constant top radius, corresponding to $R = const$ in Eqs. (3) and (4). A time-independent radius should be even more usual in the case of gold-catalyzed VLS growth [2]. Treating Eqs. (3) and (4) at $R = const$, using Eq. (1) under the standard condition $N_5 << N_3$ (Refs. [2,14,24]) and Eq. (2), we can relate $dN_3/dt$ to $d\beta/dt$ according to

$$\frac{dN_3}{dt} = \frac{\pi R^3}{\Omega_L} \frac{1}{(1+\cos\beta)^2} \frac{d\beta}{dt} . \tag{5}$$

The time-dependent nucleation rate can be presented in the form [27-29]

$$J(t) = J_* \exp\left[ -\frac{A}{\Delta\mu(t)} \right] . \tag{6}$$

Here, $A$ is the dimensionless surface energy of two-dimensional island and $\Delta\mu$ is the time-dependent chemical potential of III-V pair in liquid with respect to the reference solid state. The pre-exponential factor $J_*$ can be treated as composition-independent in the first approximation. The $\Delta\mu$ is defined as [24]

$$\Delta\mu(t) = \mu_3(t) + \mu_5(t) - \mu_{35}^0 , \tag{7}$$

with $\mu_{35}^0$ as the chemical potential of solid and $\mu_k$ as the concentration-dependent chemical potentials of group III and V atoms in liquid.

Chemical potentials in liquid are calculated within the regular solution model omitting the power terms with $c_5 << 1$ [24]

$$\mu_3(t) = \mu_3^0 + \ln[c_3(t)] + \omega_{3Au}[1 - c_3(t)]^2 ,$$
$$\mu_5(t) = \mu_5^0 + \ln[c_5(t)] + \omega_{35} c_3^2(t) + \omega_{5Au}[1 - c_3(t)]^2 + (\omega_{35} + \omega_{5Au} - \omega_{3Au}) c_3(t)[1 - c_3(t)] , \tag{8}$$

with the atomic concentrations $c_k = N_k/(N_3 + N_5 + N_{Au}) \cong N_k/(N_3 + N_{Au})$ for $k = 3$ and 5. Here, $\mu_k^0$ are chemical potentials of pure liquids and $\omega_{ik}$ are the binary interaction constants (in thermal units). In calculations, we use the parameters of gold-catalyzed GaAs NWs summarized in Table 1, for a typical growth temperature of 500 ° C [30]. The $A$ value corresponds to the effective surface energy of two-dimensional island $\gamma_{eff} = 0.23$ J/m$^2$, with regular triangle shape [17,18]. The $\Delta\mu_{GaAs}^0$ is defined according to $\Delta\mu_{GaAs}^0 = \mu_{Ga}^0 + \mu_{As}^0 - \mu_{GaAs}^0$. Now, Eqs. (3) to (8) constitute the closed system for finding the time-dependent droplet composition and contact angle under the given fluxes $v_3(t)$ and $v_5(t)$. This system can only be solved numerically; analytical approximations for the solutions will be considered elsewhere.

Table 1. Parameters of Au-Ga-As system used in calculations

| $\omega_{GaAs}$ | $\omega_{GaAu}$ | $\omega_{AsAu}$ | $\Delta\mu_{GaAs}^0$ | $\gamma_{eff}$ (J/m$^2$) | $A$ | $v_{As}^{des}$ (nm/s) | $J_*$ (1/nm$^2$s) |
|---|---|---|---|---|---|---|---|
| -4.488 | -9.517 | 1.101 | 11.80 | 0.23 | 14.6 | 37000 | 23 000 |

## 3. Results and discussion

Figure 1 shows the time evolution of the droplet contact angle from the initial value of 90°, obtained by numerically solving the model equations at a fixed $v_5 - v_3 = 3$ nm/s, two different $v_3 = 0.5$ nm/s and 1.5 nm/s, and three different GaAs NW radii $R = 20$, 40, and 80 nm, for the parameters of GaAs NWs given in Table 1. Both gallium and arsenic fluxes are turned on at $t = 0$. In the considered range of gallium fluxes, the stationary contact angle ranges between ~ 115 and ~ 120°. For a given gallium flux, saturation to the stationary value takes longer time for thicker NWs, which is explained by a larger reservoir effect in larger droplets. Increasing $v_3$ at a fixed $v_5 - v_3$ is equivalent to decreasing the V/III flux ratio $v_5 / v_3$, and yields larger stationary contact angles. For a given NW radius, higher gallium flux $v_3$ leads to a much faster increase of the contact angle and its saturation to the stationary value. This conclusion seems plausible, because inputting gallium at a higher rate should lead to a more rapid swelling of the droplet.

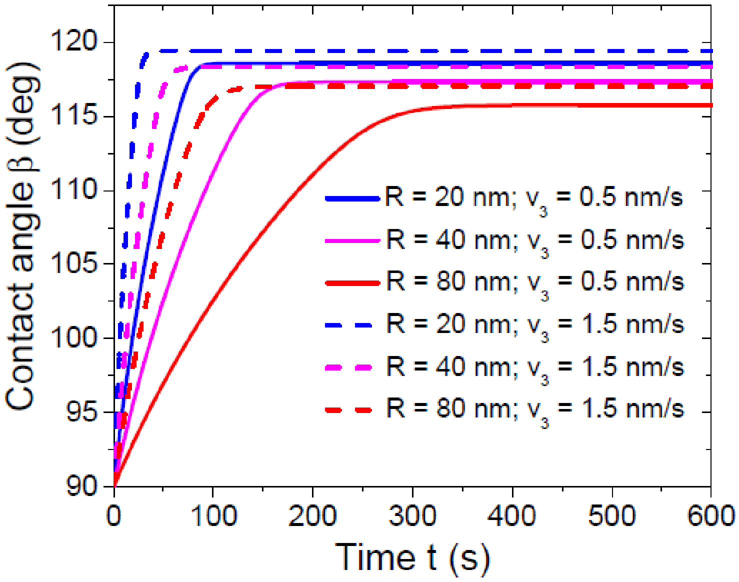

**Fig. 1.** Time evolution of the droplet contact angle from the initial state $\beta = 90^\circ$ at $t = 0$, after switching the material fluxes $v_3$ and $v_5$. The difference $v_5 - v_3$ is fixed at 3 nm/s. The gallium fluxes $v_3$ and the NW radii $R$ are given in the legend

Figure 2 shows a more interesting situation where one of the material fluxes is changed abruptly during the NW growth. Such a procedure is used during *in situ* growth monitoring in a transmission electron microscope to investigate the crystal phase selection in GaAs NWs as a function of the contact angle [22]. In the first case (loop (a) in Fig. 2), the gallium flux is fixed at 4.5 nm/s, while the arsenic flux is changed abruptly from 8.5 nm/s to either 19.5 nm/s or 6.0 nm/s, and returned to its initial value after 40 s. As expected, increase (decrease) of the arsenic flux leads to a rapid decrease (increase) of the contact angle. However, the shapes of the corresponding curves are not symmetric. In the second case (loop (b) in Fig. 2), the arsenic flux is fixed at 8.5 nm/s, while the gallium flux is changed abruptly from 4.5 nm/s to either 6.5 nm/s or 0.5 nm/s, and returned to its initial value after 86 s. Increase (decrease) of the gallium flux leads to an increase (decrease) of the contact angle. The droplet shape changes slower than under varying arsenic flux, while the shapes of the two curves becomes more symmetric compared to the first case. We note that even with these large values of material fluxes (which are more typical deposition techniques), the droplet contact angle can only be tuned within a narrow range of 113-120°. This may suggest a strong influence of re-emitted species [28] and in any case requires further study. The curves shown in Fig. 2 clearly demonstrate that a very similar effect on the droplet contact angle can be achieved by modifying either group V or group III flux.

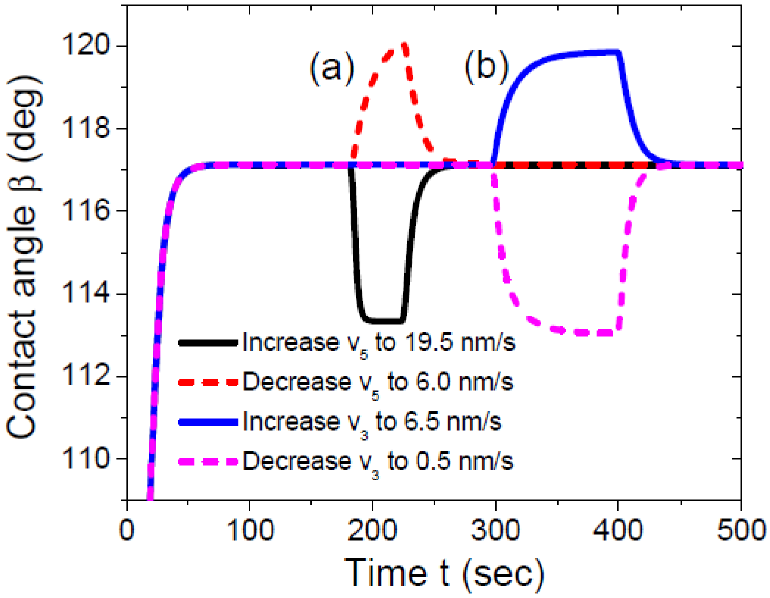

**Fig. 2.** Contact angle versus time at (a) variable $v_5$ which is changed abruptly from $v_5^0 = 8.5$ nm/s to 19.5 nm/s (solid line) or 6.0 nm/s (dashed line) for 40 s and then returned abruptly to its initial value, at a fixed $v_3^0 = 4.5$ nm/s; and (b) variable $v_3$ which is changed abruptly from $v_3^0 = 4.5$ nm/s to 6.5 nm/s (solid line) or 0.5 nm/s (dashed line) for 86 s and then returned abruptly to its initial value, at a fixed $v_5^0 = 8.5$ nm/s. The value $R$ of GaAs NW radius is fixed at 20 nm

In conclusion, we have presented a model for non-stationary droplet shape during the VLS growth of III-V NWs under varying materials inputs. It captures the main ingredients of this non-stationary process, including the ability to quickly inflate or shrink the droplet by abruptly changing one of the two material fluxes, and then retain its initial shape. This can be very useful for understanding and controlling the crystal phase switching of GaAs and other III-V NWs, and possibly to minimize the faulted polytypic regions in the WZ-to-ZB phase transitions. We now plan to model the experimentally measured shapes of the droplet within the frame of the model.

***Acknowledgements.*** *The authors thank the Russian Science Foundation for financial support under the Grant 19-72-30004.*

## References

[1] Zhang A, Zheng G, Lieber CM. *Nanowires: Building blocks for nanoscience and nanotechnology*. Springer; 2016.

[2] Dubrovskii VG. Theory of VLS growth of compound semiconductors. In: Morral AF, Dayeh SA, Jagadish C. (eds.) *Semiconductor Nanowires I: Growth and Theory, Volume 93*. 1st ed. Burlington: Academic Press; 2015. p.1-78.

[3] Glas F. Critical dimensions for the plastic relaxation of strained axial heterostructures in free-standing nanowires. *Physical Review B*. 2006;74(12): 121302 (R).

[4] Ng KW, Ko WS, Tran TTD, Chen R, Nazarenko MV, Lu F, Dubrovskii VG, Kamp M, Forchel A, Chang-Hasnain CJ. Unconventional growth mechanism for monolithic integration of III–V on silicon. *ACS Nano*. 2013;7(1): 100-107.

[5] Cirlin GE, Dubrovskii VG, Petrov VN, Polyakov NK, Korneeva NP, Demidov VN, Golubok AO, Masalov SA, Kurochkin DV, Gorbenko OM, Komyak NI, Ustinov VM, Egorov AY, Kovsh AR, Maximov MV, Tsatusul'nikov AF, Volovik BV, Zhukov AE, Kop'ev PS, Alferov ZI, Ledentsov NN, Grundmann M, Bimberg D. Formation of InAs quantum dots on a silicon (100) surface. *Semiconductor Science & Technology*. 1998;13(1): 1262-1265.

[6] Wagner RS, Ellis WC. Vapor liquid solid mechanism of single crystal growth. *Applied Physics Letters*. 1964;4: 89.

[7] Dubrovskii VG, Sibirev NV, Suris RA, Cirlin GE, Harmand JC, Ustinov VM. Diffusion-controlled growth of semiconductor nanowires: vapor pressure versus high vacuum deposition. *Surface Science*. 2007;601(18): 4395-4401.

[8] Dubrovskii VG, Sibirev NV, Cirlin GE. Kinetic model of the growth of nanodimensional whiskers by the vapor-liquid-crystal mechanism. *Technical Physics Letters*. 2004;30(8): 682-686.

[9] Dubrovskii VG, Soshnikov IP, Sibirev NV, Cirlin GE, Ustinov VM. Growth of GaAs nanoscale whiskers by magnetron sputtering deposition. *Journal of Crystal Growth*. 2006;289(1): 31-36.

[10] Dubrovskii VG, Soshnikov IP, Cirlin GE, Tonkikh AA, Samsonenko YB, Sibirev NV, Ustinov VM. On the non-monotonic lateral size dependence of the height of GaAs nanowhiskers grown by molecular beam epitaxy at high temperature. *Physica Status Solidi B*. 2004;241(7): R30-R33.

[11] Colombo C, Spirkoska D, Frimmer M, Abstreiter G, Morral AF. Ga-assisted catalyst-free growth mechanism of GaAs nanowires by molecular beam epitaxy. *Physical Review B*. 2008;77(15): 155326.

[12] Gibson SJ, Boulanger JP, LaPierre RR. Opportunities and pitfalls in patterned self-catalyzed GaAs nanowire growth on silicon. *Semiconductor Science & Technology*. 2013;28(10): 105025.

[13] Matteini F, Dubrovskii VG, Rüffer D, Tütüncüoğlu G, Fontana Y, Morral AF. Tailoring the diameter and density of self-catalyzed GaAs nanowires on silicon. *Nanotechnology*. 2015;26(10): 105603.

[14] Dubrovskii VG. *Nucleation theory and growth of nanostructures*. Berlin: Springer; 2014.

[15] Dheeraj DL, Munshi AM, Scheffler M, Van Helvoort ATJ, Weman H, Fimland BO. Controlling crystal phases in GaAs nanowires grown by Au-assisted molecular beam epitaxy. *Nanotechnology*. 2013;24(1): 015601.

[16] Akopian N, Patriarche G, Liu L, Harmand JC, Zwiller V. Crystal phase quantum dots. *Nano Letters*. 2010;10(4): 1198–1201.

[17] Glas F, Harmand JC, Patriarche G. Why does wurtzite form in nanowires of III-V zinc-blende semiconductors? *Physical Review Letters*. 2007;99(14): 146101.

[18] Dubrovskii VG, Sibirev NV, Harmand JC, Glas F. Growth kinetics and crystal structure of semiconductor nanowires. *Physical Review B*. 2008;78(23): 235301.

[19] Johansson J, Karlsson LS, Dick KA, Bolinsson J, Wacaser BA, Deppert K, Samuelson L. Effects of supersaturation on the crystal structure of gold seeded III−V nanowires. *Crystal Growth & Design*. 2009;9(2): 766-773.

[20] Ross FM. Controlling nanowire structures through real time growth studies. *Reports on Progress in Physics*. 2010;73(11): 114501.

[21] Wen CY, Tersoff J, Hillerich K, Reuter MC, Park JH, Kodambaka S, Stach EA, Ross FM. Periodically changing morphology of the growth interface in Si, Ge, and GaP nanowires. *Physical Review Letters*. 2011;107(2): 025503.

[22] Jacobsson D, Panciera F, Tersoff J, Reuter MC, Lehmann S, Hofmann S, Dick KA, Ross FM. Interface dynamics and crystal phase switching in GaAs nanowires. *Nature*. 2016;531: 317-322.

[23] Dubrovskii, VG. Development of growth theory for vapor-liquid-solid nanowires: contact angle, truncated facets and crystal phase. *Crystal Growth & Design*. 2017;17(5): 2544-2548.

[24] Dubrovskii VG, Sokolova ZV, Rylkova MV, Zhiglinsky AA. Composition and contact angle of Au-III-V droplets on top of Au-catalyzed III-V nanowires. *Materials Physics and Mechanics*. 2018;36(1): 1-7.

[25] Glas F. Vapor fluxes on the apical droplet during nanowire growth by molecular beam epitaxy. *Physica Status Solidi B*. 2010;247(2): 254-258.

[26] Kim W, Dubrovskii VG, Vukajlovic-Plestina J, Tütüncüoglu G, Francaviglia L, Güniat L, Potts H, Friedl M, Leran JB, Morral AF. Bi-stability of contact angle and its role in achieving quantum-thin self-assisted GaAs nanowires. *Nano Letters*. 2018;18(1): 49-57.

[27] Dubrovskii VG. Nucleation and growth of adsorbed layer: self-consistent approach based on Kolmogorov-Avrami model. *Physica Status Solidi B*. 1992;171(2): 345-356.

[28] Glas F, Ramdani MR, Patriarche G, Harmand JC. Predictive modeling of self-catalyzed III-V nanowire growth. *Physical Review B.* 2013;88(19): 195304.

[29] Dubrovskii, VG, Grecenkov J. Zeldovich nucleation rate, self-consistency renormalization, and crystal phase of Au-catalyzed GaAs nanowires. *Crystal Growth & Design*. 2015;15(1): 340-347.

[30] Leshchenko ED, Ghasemi M, Dubrovskii VG, Johansson J. Nucleation-limited composition of ternary III-V nanowires forming from quaternary gold based liquid alloys. *CrystEngComm*. 2018;20: 1649-1655.